

HEDL-SA-902

CONF-750607-55

MASTER

MODE OF FAILURE OF LMFBR FUEL PINS

D. F. Washburn

For presentation at the meeting
of the American Nuclear Society
New Orleans, Louisiana, June 8-13, 1975

NOTICE

PORTIONS OF THIS REPORT ARE ILLEGIBLE. It
has been reproduced from the best available
copy to permit the broadest possible avail-
ability.

This paper is based on work performed at HANFORD ENGINEERING DEVELOPMENT LABORATORY, Richland, Washington, operated by Westinghouse Hanford Company, a subsidiary of Westinghouse Electric Corporation for the UNITED STATES ENERGY RESEARCH AND DEVELOPMENT ADMINISTRATION UNDER CONTRACT AT(45-1)-2170.

NOTICE

This report was prepared as an account of work sponsored by the United States Government. Neither the United States nor the United States Energy Research and Development Administration, nor any of their employees, nor any of their contractors, subcontractors, or their employees, makes any warranty, express or implied, or assumes any legal liability or responsibility for the accuracy, completeness or usefulness of any information, apparatus, product or process disclosed, or represents that its use would not infringe privately owned rights.

DISTRIBUTION OF THIS DOCUMENT IS UNLIMITED

DISCLAIMER

This report was prepared as an account of work sponsored by an agency of the United States Government. Neither the United States Government nor any agency thereof, nor any of their employees, makes any warranty, express or implied, or assumes any legal liability or responsibility for the accuracy, completeness, or usefulness of any information, apparatus, product, or process disclosed, or represents that its use would not infringe privately owned rights. Reference herein to any specific commercial product, process, or service by trade name, trademark, manufacturer, or otherwise does not necessarily constitute or imply its endorsement, recommendation, or favoring by the United States Government or any agency thereof. The views and opinions of authors expressed herein do not necessarily state or reflect those of the United States Government or any agency thereof.

DISCLAIMER

Portions of this document may be illegible in electronic image products. Images are produced from the best available original document.

MODE OF FAILURE OF LMFBR FUEL PINS

The original objectives of the PNL-5 (X114) irradiation test were to evaluate mixed-oxide fuel performance and to confirm the design adequacy of the FFTF fuel pins. After attainment of the initial objectives the irradiation of several of the original fuel pins was continued until a cladding breach occurred. The cladding of one fuel pin developed a fissure at 13.1 a/o burnup.

At the onset of the irradiation test, the PNL-5 subassembly contained 37 mixed-oxide fuel pins clad with solution-annealed 304 stainless steel. (The FFTF reference cladding was subsequently changed to 20% cold-worked 316 stainless steel to avoid irradiation-enhanced swelling.) Details of the fabrication and irradiation parameters are shown in the first slide. The 13-1/2 inch-long fuel column contained mixed-oxide fuel pellets with a composition of 75% UO_2 and 25% PuO_2 and an O/M ratio of 1.99. The planar smear density was 88%. The fuel pin diameter was 0.250 inch and the cladding thickness was 0.016 inch.

The consequences of a cladding breach were evaluated by reconstituting the original 37-pin subassembly into two 19-pin subassemblies after a burnup at 50,000 MWd/MTM (5.2 a/o). The original pins were supplemented with fresh pins as necessary. Irradiation of the subassemblies was continued until a cladding breach occurred.

The first cladding breach occurred in the PNL-5A subassembly which contained 19 of the original 37 pins. The failed fuel pin was later identified as a corner pin in the 19-pin subassembly, slide 2. The cladding breach, occurring at a burnup of 128,000 MWd/MTM (13.1 atom percent), was characterized by a gradual release of fission gas to the reactor cover gas. No other evidence of the cladding fissure was detected and subsequent examination showed the fission gas release was through a microscopic fissure in the cladding 3.5 inches below the top of the fuel column. The nature of the fissure can best be described as benign.

Characteristics of the fuel pin at the time of failure are shown in slide 3. The gas pressure at the time of failure was calculated to be 1140 psi. This resulted from the release of 97% of the available fission gas or 204 cc. The maximum inner-surface cladding temperature at the top of the fuel column was 920°F.

Removal of the hex duct at HFEF showed several of the fuel pins along one edge of the bundle (including the breached pin) were severely distorted. The distortion was most severe just above the core midplane and is evident in the photograph shown in the fourth slide. This photograph (supplied by ANL) shows the pin in position 12 has been displaced to position 7 while the pin in position 11 is in position 12. The pin arrangement shown earlier clarifies this rearrangement, Slide 5. As a result of this distortion, conditions were favorable for pin-to-pin contact. The cause of the distortion was not evident from an examination of either the fuel pins or the subassembly hardware although the metallographic examination of PNL 5-2, a neighbor to the breached pin suggests it occurred during assembly of the PNL-5A subassembly.

The cladding on the side of fuel pin PNL 5-2 nearest the hex duct contained a deep gouge over a length of about one inch with intermittent depths as much as 0.007 inch, Slide 6. A longitudinal section through this gouge showed the direction of metal flow was downward, Slide 7, suggesting it was caused when the hex duct was lowered into place during reconstitution of the bowed fuel pins from the original PNL-5 subassembly. It is believed that twisted pins forced pin 5-2 into a position where it was subjected to high axial forces necessary to produce the gouge.

Gamma-scanning and weight measurements at HFEF positively identified the breached fuel pin as PNL 5-1. This was one of the severely distorted pins observed earlier although there was no outward evidence of the cladding breach. No other breached pins were present in the subassembly.

The cladding strains for the breached fuel pin and for PNL 5-2, a sibling pin, were obtained from diameter measurements and immersion density measurements. The fuel pin diameter was measured with a micrometer at discrete locations along the fuel pin. At these same locations, the cladding density was measured. The density measurements provided a means of calculating the diameter increase due to irradiation swelling. Inelastic strain of the cladding is the total diameter increase (micrometer measurements) and the diameter increase due to swelling (density measurements). The results from these measurements for the breached

pin, PNL 5-1, and for its sibling, PNL 5-2, are shown in Slide 8. The inelastic strain at the fissure was 1.1% and the maximum inelastic strain in PNL 5-1 was 1.2%. The maximum inelastic strain in PNL 5-2 was 1.0%.

The mechanism of failure in the cladding was determined by incrementally polishing and examining numerous transverse surfaces in a section of the fuel pin known to contain the cladding breach. An area of cladding within an included angle of about 30° and extending axially for about 5/8-inch contained a high density of intergranular porosity and cracking. A typical example of these features is shown in Slide 9. There was no single surface which contained a continuous through crack; suggesting the cladding breach resulted from interconnection of the intergranular porosity. This intergranular porosity was not observed in any other area of the cladding of the breached pin or its sibling, PNL 5-2, or in the cladding of PNL 5-34 which was examined at the suspect axial height. The pin which is suspected of being in contact with the failed pin is now undergoing examination.

Cladding thickness measurements around the circumference of the cladding in several transverse surfaces of the breach sample were used to verify the visual indication of localized deformation in the region of grain boundary porosity. The maximum local deformation in the region of grain boundary porosity was 8%, the intergranular porosity and cladding necking were interpreted as evidence that the cladding breach was the result of thermal creep which occurred because of pin-to-pin contact between PNL 5-1 and one of its neighbors.

An additional indication of a "hot spot" in the cladding was the intergranular penetration of fission-product palladium at the inner surface of the cladding which was confined to the area of the intergranular porosity, Slide 10. The depth of penetration was about 50 microns. Elsewhere in the breached pin and in its sibling the palladium deposit had a uniform thickness of about five microns with no evidence of intergranular penetration, Slide 11. There was no indication that the intergranular penetration of palladium contributed to the failure but it does suggest that locally higher temperatures did exist in the cladding. The

uniform layer of palladium was profusely cracked but there was no other indication of cladding attack at the inner surface.

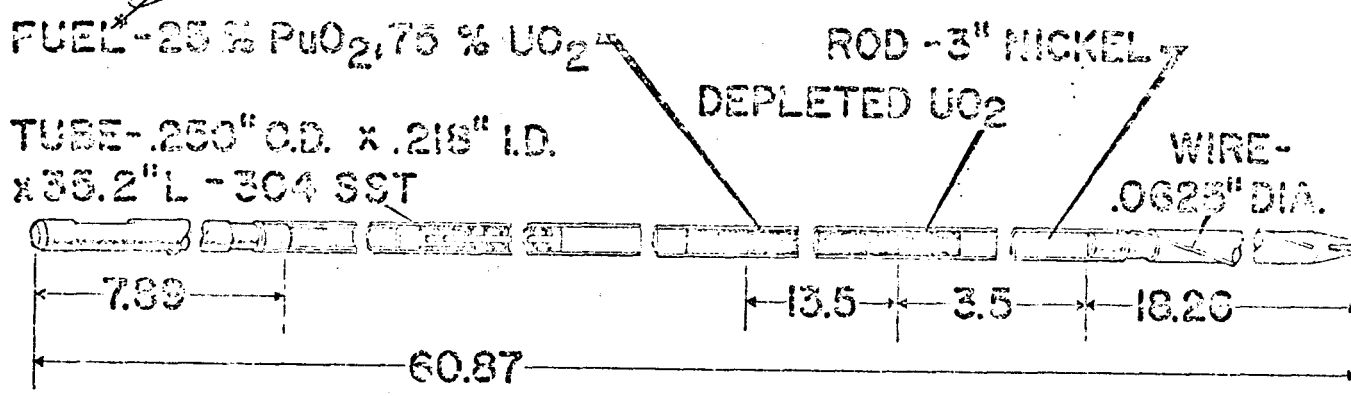
The intergranular porosity, local deformation of the cladding, and intergranular penetration of palladium at the cladding inner surface provides strong evidence that the cladding fissure resulted from thermal creep which was confined to a hot spot in the cladding. The 900°F nominal cladding temperature is too low for thermal creep. However, calculations by M. Parker showed that restricted coolant flow resulting from pin-to-pin contact could cause a cladding hot spot approaching 1200°F. A temperature increase of this magnitude is sufficient to result in thermal creep of the cladding. Under conditions of pin-to-pin contact at full power the pin survived 376 Equivalent Full Power Days (7.9 a/o burnup) before the occurrence of a benign cladding breach.

Fabrication and Irradiation Parameters for PNL 5
Fuel P, NC

~~APPENDIX 10
Fabrication and Irradiation Parameters for PNL 5~~

~~(Fuel Pin Design)~~

~~BBF 2, PNL 5~~



Plenum : Fuel Volume 1:1

Pin Power 12 kw/ft

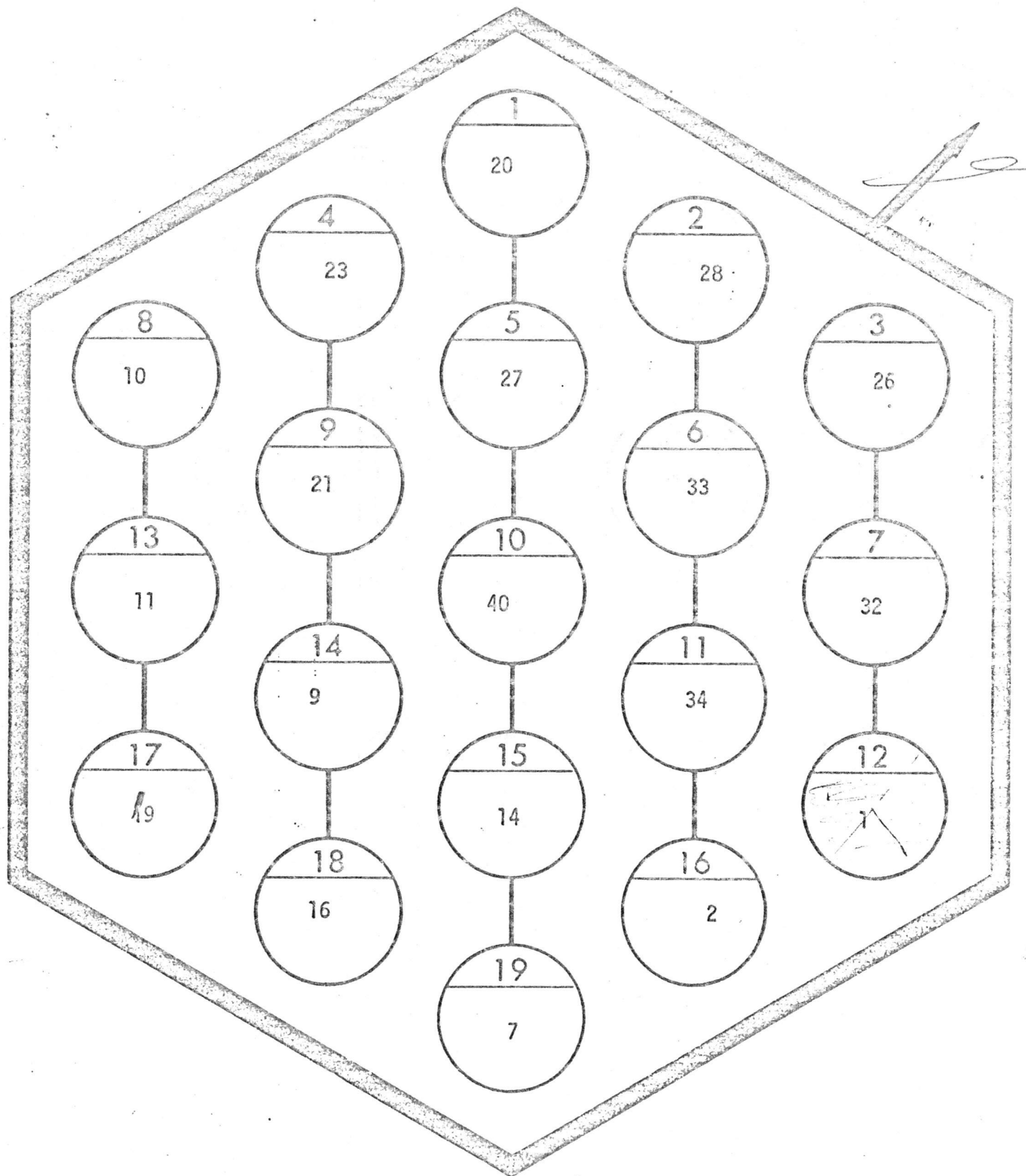
Max. Cladding Temp 920°F

Fuel O/M 1.99

Planar smear density 88%

X114 PNL-5A
Charged: 4/22/71 Run 48D
Grid Position 6C3

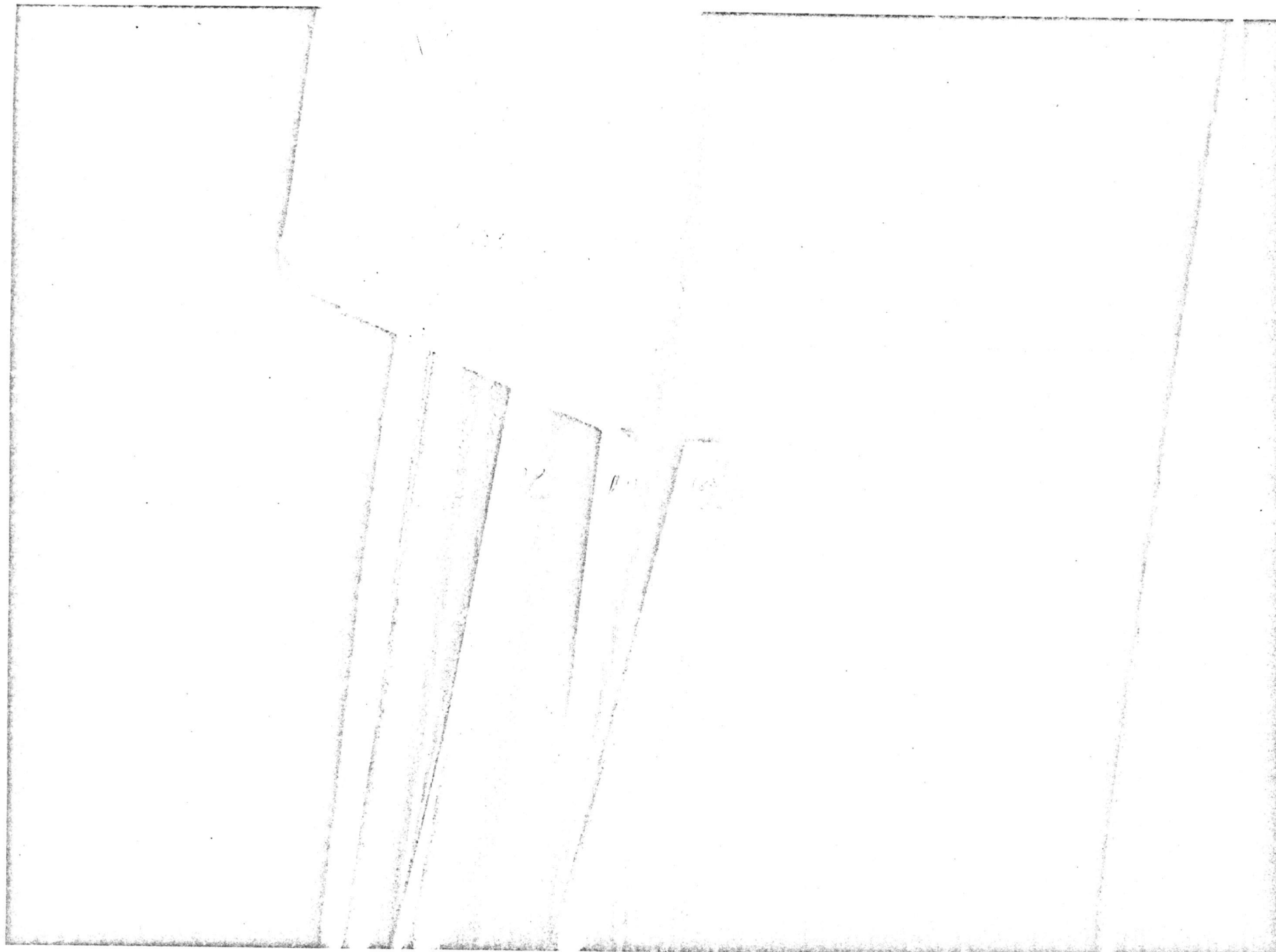
Exposure: X054 11106 MWD



PNL 5A Subassembly Arrangement

CHARACTERISTICS OF PNL-5-1
AT TIME OF CLADDING BREACH

Fluence, nvt ($\epsilon > 0.1 \text{ mev}$)	8.6×10^{22}
Burnup	128 MWd/kg 13.1 atom percent
Gas Release	
cc	204
percent	97
Gas Pressure	1170 psi
Max Cladding Temperature	920°F
Coolant Temperature	840°F
Location of Fissure from Top of Fuel Column	3.15 inches

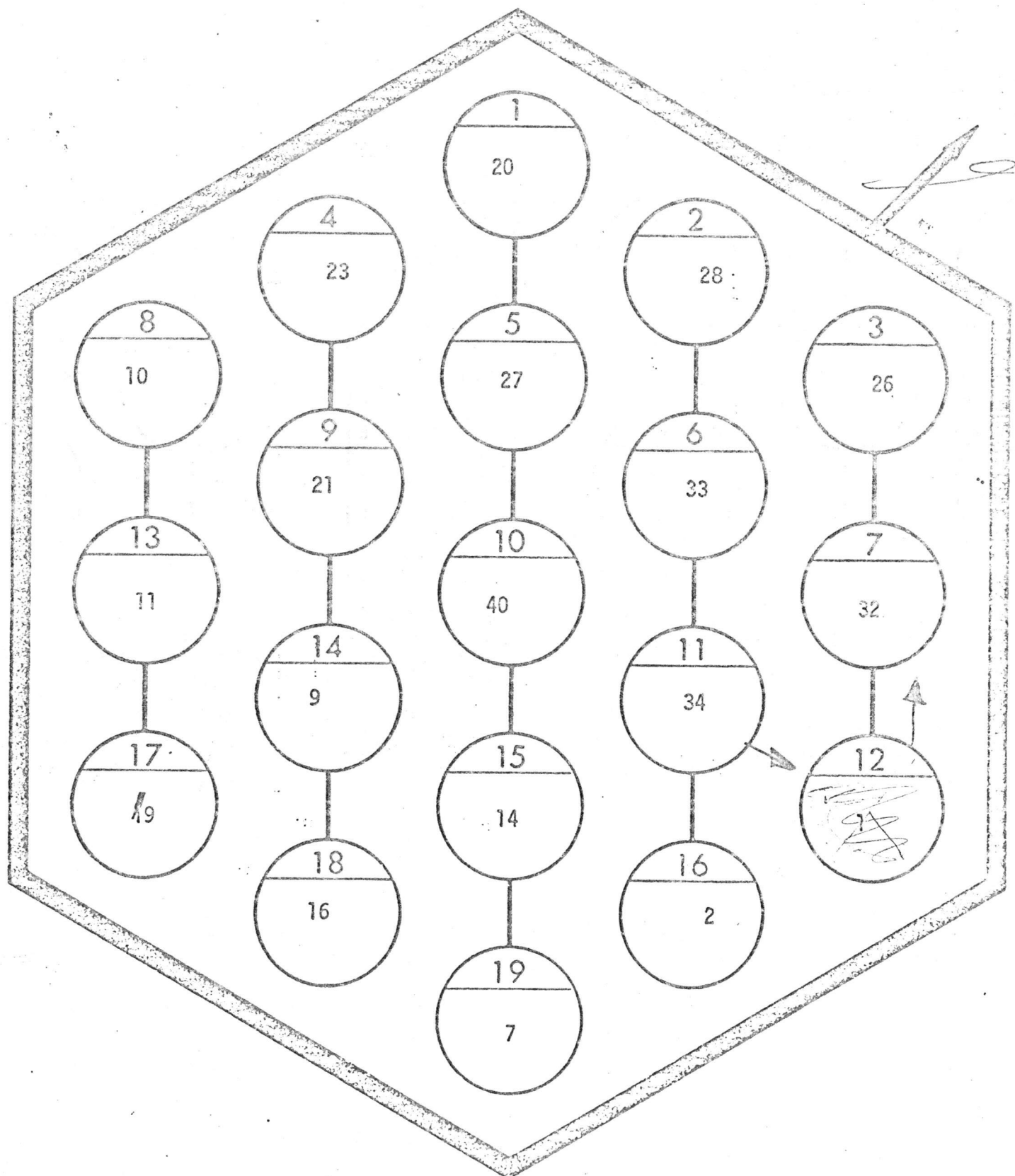


PNL 5A Disassembly

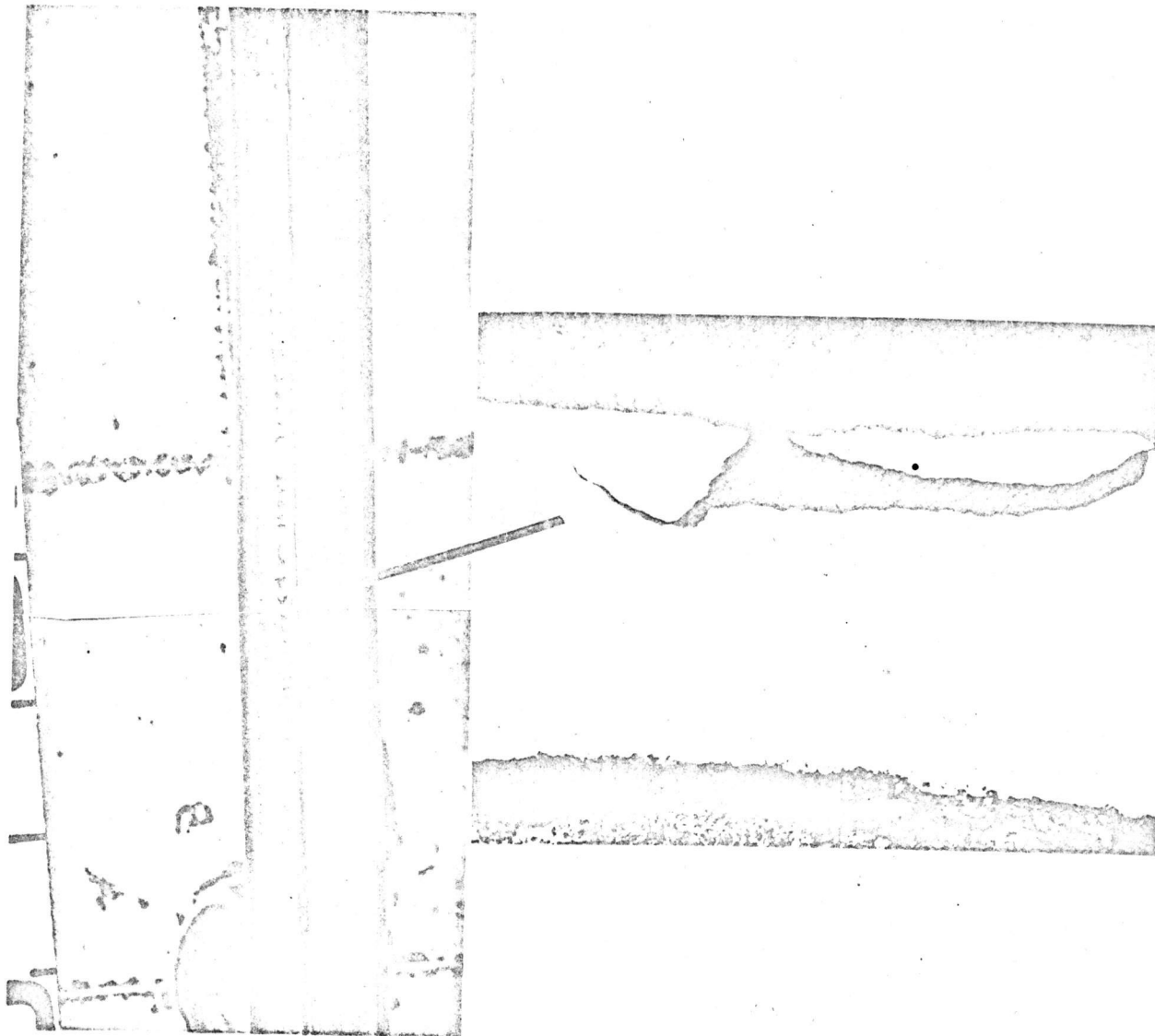
(ANL photograph)

X114 PNL-5A
Charged: 4/22/71 Run 48D
Grid Position 6C3

Exposure: X054 11106 MWD

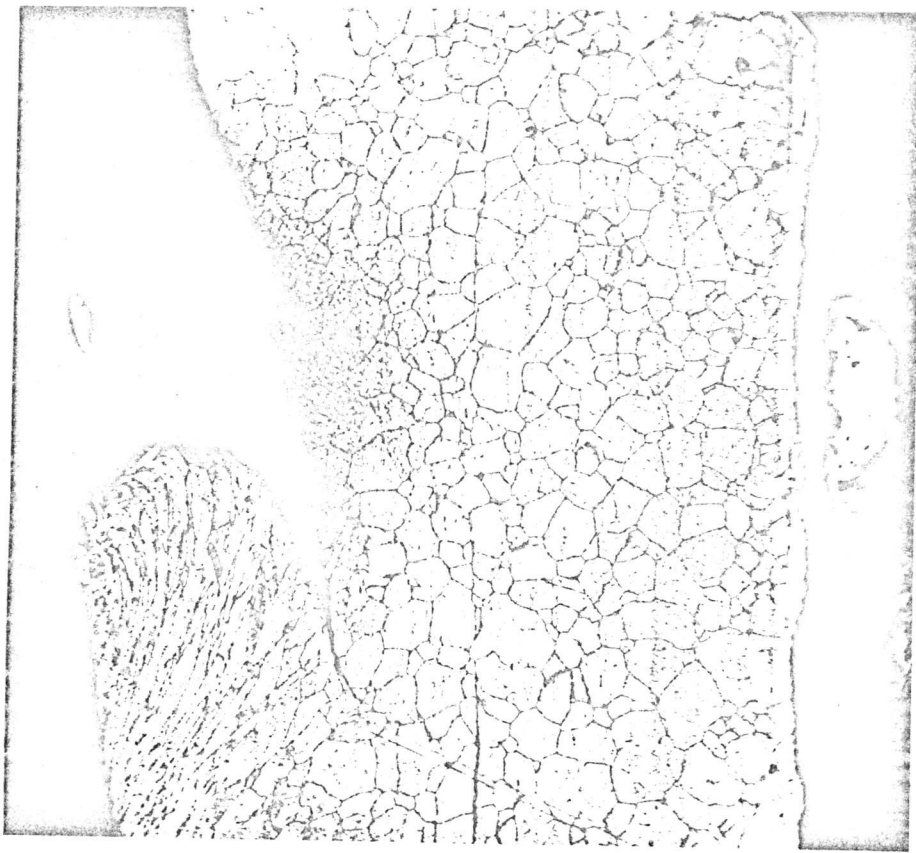


PNL 5A Subassembly Arrangement



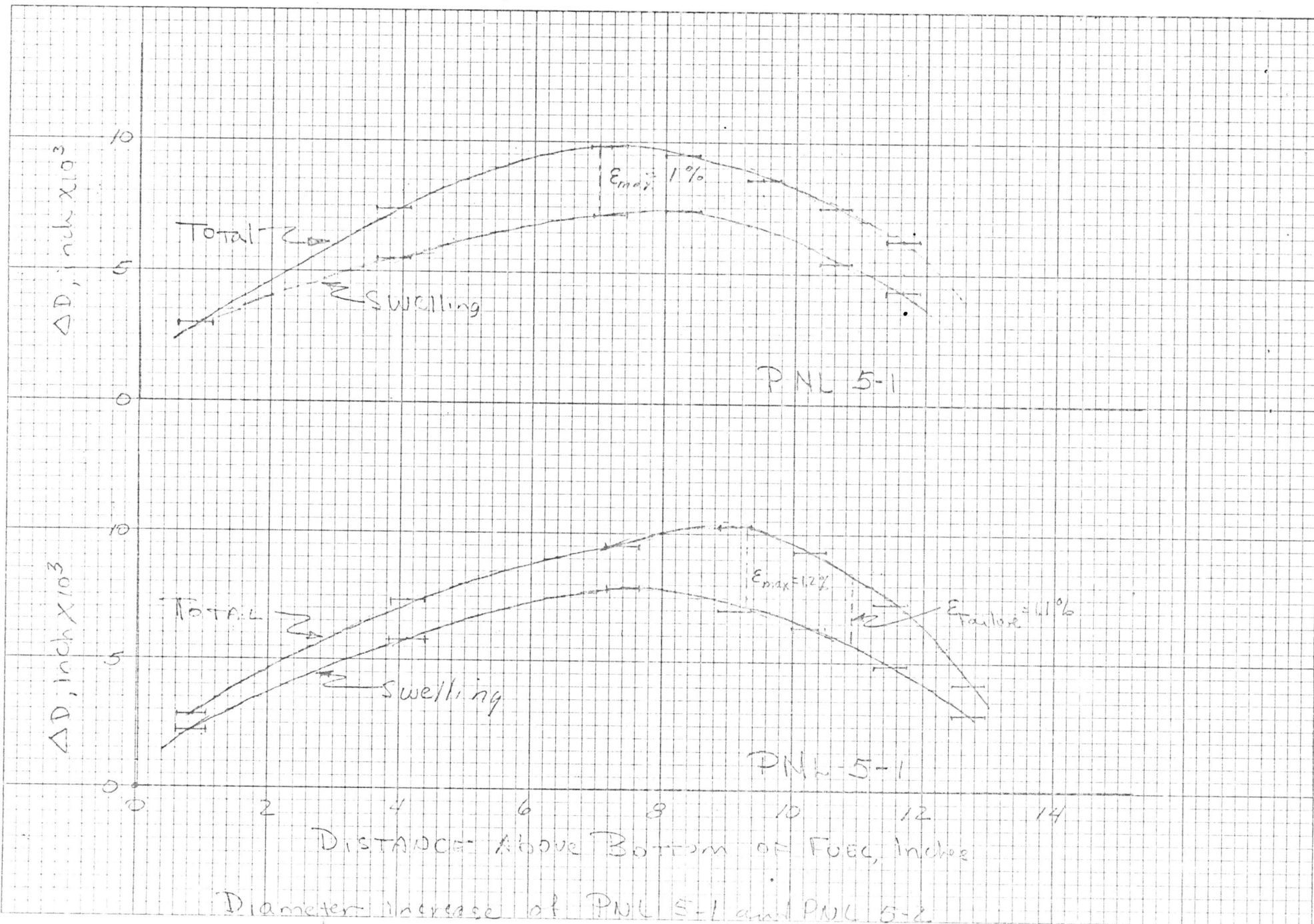
Gouge on outer surface of PNL 5-2. Macroscopic appearance and a transverse-surface micrograph.

TOP OF FUEL PIN

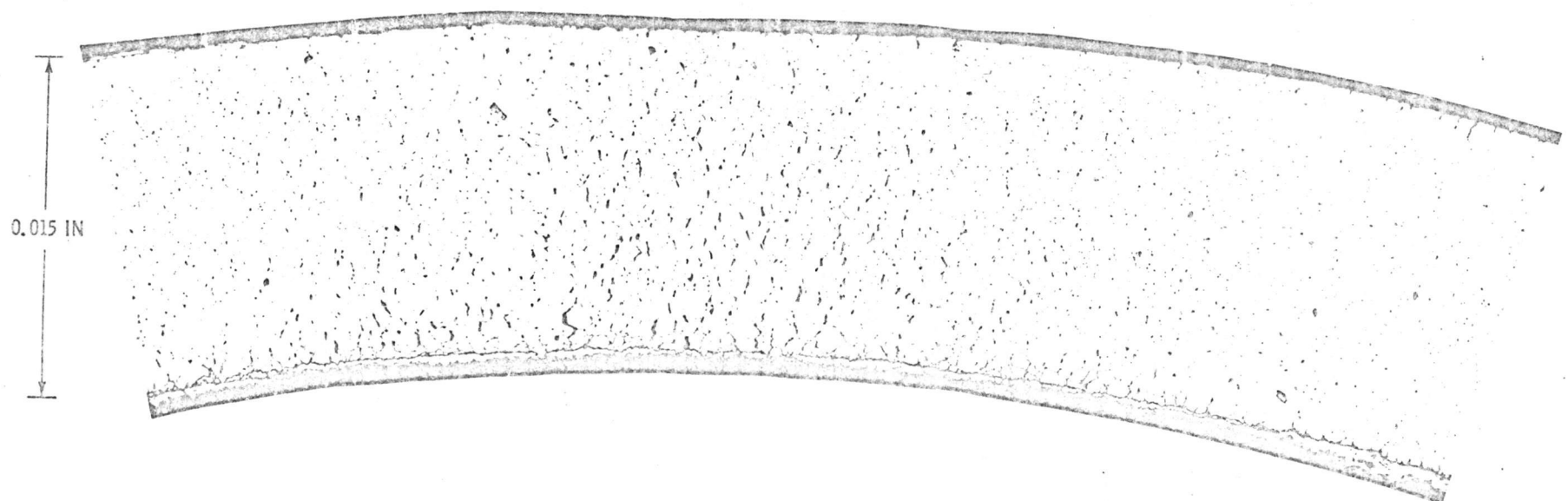


5 MILS

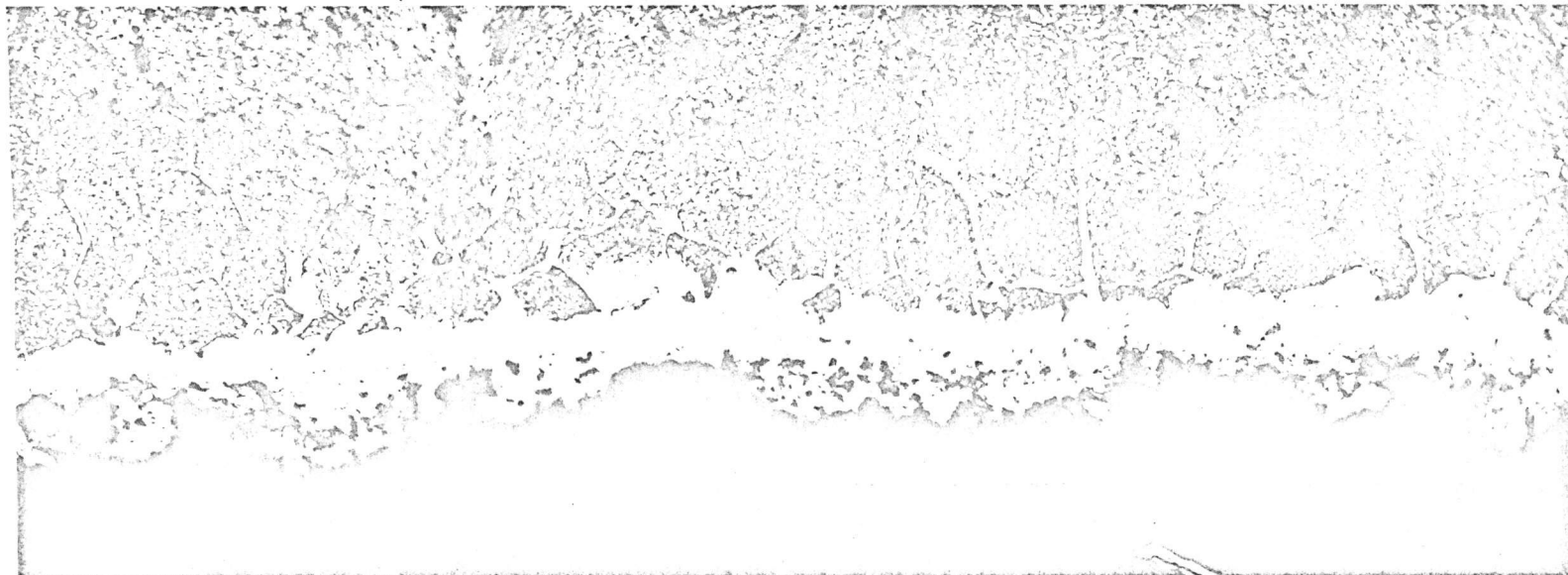
LONGITUDINAL Section through the
Gouge on PNL 5-2



CLADDING BREACH
PNL 5-1



HEDL 7503-99.2



1 MIL

Intergranular Penetration of palladium on inner surface of
cladding at the breach site in PNL S-1.



Uniform layer of fission-product palladium on inner
surface of cladding of PNL 5-1 and PNL 5-2